Clinical and Translational Radiation Oncology 51 (2025) 100906

Contents lists available at ScienceDirect

Clinical and Translational Radiation Oncology

journal homepage: www.sciencedirect.com/journal/clinical-and-translational-radiation-oncology

Original Research Article

Neoadjuvant chemoradiotherapy up-regulates PD-L1 in radioresistant colorectal cancer

Sung Uk Bae [a,b,c,1], Hye Won Lee [c,d,1], Jee Young Park [a,d,e,f,1], Incheol Seo [g], Jae-Min Cho [a,d], Jin Young Kim [h], Ju Yup Lee [i], Yoo Jin Lee [i], Seong Kyu Baek [a], Nam Kyu Kim [j], Sang Jun Byun [c,e,*], Shin Kim [c,f,**]

[a] Department of Surgery, School of Medicine, Keimyung University and Dongsan Hospital, Daegu, Republic of Korea
[b] Department of Medicine, The Graduate School, Yonsei University, Seoul, Republic of Korea
[c] Institute of Medical Science & Institute for Cancer Research, Keimyung University, Daegu, Republic of Korea
[d] Department of Pathology, School of Medicine, Keimyung University and Dongsan Hospital, Daegu, Republic of Korea
[e] Department of Radiation Oncology, School of Medicine, Keimyung University and Dongsan Hospital, Daegu, Republic of Korea
[f] Department of Immunology, School of Medicine, Keimyung University, Daegu, Republic of Korea
[g] Department of Immunology, Kyungpook National University School of Medicine, Daegu, Republic of Korea
[h] Division of Hematology and Oncology, Department of Internal Medicine, School of Medicine, Keimyung University and Dongsan Hospital, Daegu, Republic of Korea
[i] Division of Gastroenterology and Hepatology, Department of Internal Medicine, School of Medicine, Keimyung University and Dongsan Hospital, Daegu, Republic of Korea
[j] Division of Colorectal Surgery, Department of Surgery, Severance Hospital, Colorectal Cancer Clinic, Yonsei University College of Medicine, Seoul, Republic of Korea

ARTICLE INFO

Keywords:
Locally advanced rectal cancer
PD-L1
Chemoradiotherapy
Immune checkpoint inhibitors

ABSTRACT

Background: Combining radiotherapy (RT) with immune checkpoint inhibitors (ICIs) is a promising strategy that can enhance the therapeutic efficacy of ICIs. However, little is known about RT-induced changes in the expression of immune checkpoints, such as PD-L1, and their clinical implications in colorectal cancer (CRC). This study aimed to investigate the association between responsiveness to RT and changes in PD-L1 expression in human CRC tissue and cell lines.

Methods: Tissue specimens from preoperative biopsy via sigmoidoscopy and surgical resection were obtained from 24 patients with locally advanced rectal cancer (LARC) who underwent neoadjuvant chemoradiation therapy (CRT) between August 2016 and December 2017. Immunohistochemistry for PD-L1 in formalin-fixed paraffin-embedded tissue was performed from the endoscopic biopsy and surgical specimens. RNA sequencing was performed using 11 pairs of human LARC tissues before and after irradiation. After exposing human CRC cells to radiation, we investigated changes in the expression levels of PD-L1 and its regulatory signaling pathways.

Results: Patients were classified by tumor regression grade into responders (grade 2; 9 patients, 37.5 %) and non-responders (grades 3, 4, or 5; 15 patients, 62.5 %). In the non-responder group, 13 patients had low PD-L1 expression, but neoadjuvant CRT increased PD-L1 expression in 7 patients (53.9 %) (McNemar's test, p=0.034). CRT up-regulated PD-L1 in non-responder LARC tissues. Similarly, radiation increased PD-L1 in radioresistant DLD-1 cells more than in radiosensitive HCT116 cells, also affecting PD-L1-regulating genes and immune checkpoints in CRC cells. Conventional fractionated radiation treatment further increased PD-L1 in DLD-1 cells compared to HCT116 cells.

Abbreviations: RT, radiotherapy; ICIs, immune checkpoint inhibitors; CRC, colorectal cancer; LARC, locally advanced rectal cancer; CRT, chemoradiation therapy; neoCRT, neoadjuvant chemoradiotherapy; TME, tumor microenvironment; PD-L1, programmed cell death ligand-1; IHC, immunohistochemistry; FFPE, formalin-fixed paraffin-embedded; 5FU, 5-fluorouracil; CT, computed tomography; CEA, carcinoembryonic antigen; MSI, microsatellite instability; XTT, 2,3-bis (2-methoxy-4-nitro-5-sulphonyl)- 2H-tetrazolium-5-carboxanilide.

* Corresponding author at: Department of Radiation Oncology, School of Medicine, Keimyung University and Dongsan Hospital, 1095 Dalgubeol-Daero, Dalseo-Gu, Daegu 42601, Republic of Korea.

** Corresponding author at: Department of Immunology, School of Medicine, Keimyung University, 1095 Dalgubeol-Daero, Dalseo-Gu, Daegu 42601, Republic of Korea.

E-mail addresses: kryph@dsmc.or.kr (S.J. Byun), god98005@dsmc.or.kr (S. Kim).

[1] These authors contributed equally to this work.

https://doi.org/10.1016/j.ctro.2024.100906
Received 18 July 2024; Received in revised form 14 December 2024; Accepted 20 December 2024
Available online 22 December 2024

Conclusions: This study demonstrated that radiation induces an increase in PD-L1 expression, which is more pronounced in radioresistant CRC, proving the theoretical framework for a combined treatment strategy with a PD-L1 blockade for locally advanced rectal cancer.

1. Introduction

Neoadjuvant chemoradiotherapy (neoCRT) for locally advanced rectal cancer (LARC) enhances tumor downstaging, sphincter preservation, and local control [1–4]. Radiotherapy (RT) causes DNA double-strand breaks [5,6] and induces immuno-oncologic changes such as increased neo-antigen levels, tumor-infiltrating lymphocytes, and systemic antitumor effects [7–9], which are crucial in multimodal cancer treatment. Despite CRT's benefits, resistance occurs, necessitating strategies to improve outcomes. The tumor microenvironment's (TME) immune checkpoint expression, particularly programmed cell death ligand-1 (PD-L1), inhibits T cell-mediated immunity and is a key anticancer target [10]. PD-L1 upregulation in the TME improves the response and efficacy of immune checkpoint blockade [11–14]. Therefore, there is a need for studies on cancer therapy combining PD-L1 upregulation with PD-L1 blockade. Studies have revealed that neoCRT and RT induce up-regulation of PD-L1 on tumor cells [13,15–17]. However, because there are many side effects and low response rates to PD-L1 blockade [11,18], combination therapy should be considered. Therefore, we aimed to establish an appropriate anti-PD-L1 antibody treatment strategy by characterizing neoCRT-associated PD-L1 upregulation in LARC tissue and colorectal cancer (CRC) cells.

2. Materials and methods

2.1. Patients and sample collection

Tissue specimens from 24 patients with stage 2–3 rectal adenocarcinoma who underwent neoadjuvant chemoradiotherapy (CRT) between August 2016 and December 2017 were collected for immunohistochemistry (IHC). Pre-CRT samples were collected by colonoscopic biopsy and post-CRT samples were collected by surgery.

RNA sequencing (RNA-seq) samples were obtained from 11 patients [19]. Exclusion criteria included distant metastasis, hereditary syndromes, previous cancers, and patient refusal or loss to follow-up. All patients received fluorouracil-based long-course therapy and underwent various re-staging work-up before curative surgery within 6–8 weeks after CRT.

2.2. Evaluation parameters

Patient age, sex, body mass index, tumor location, and preoperative carcinoembryonic antigen (CEA) levels were recorded. Additionally, these factors were evaluated: American Joint Committee on Cancer (AJCC) tumor, node, metastasis (TNM) classification, histology, tumor budding, lymphovascular invasion, perineural invasion, extranodal extension, as well as *KRAS* and *BRAF* mutations. Primary tumor regression grade (TRG) was defined according to the Mandard regression grading system [20]. Patients were divided into two groups based on TRG: responder (TRG1/2) and non-responder (TRG3/4/5).

2.3. Immunohistochemistry

All human primary rectal cancer tissue samples were FFPE, and tissue microarrays were constructed from these specimens. PD-L1 staining was performed using a BenchMark ULTRA automated system(Ventana Medical Systems, Inc., Tucson, AZ, USA) with rabbit polyclonal PD-L1 (1:400, AnaSpec, Fremont, CA, USA) as the primary antibody. Bound antibodies were evaluated using an UltraView Universal DAB Detection Kit (Ventana Medical Systems, Inc., Tucson, AZ, USA). Placenta and tonsil tissues served as positive controls, and slides without the primary antibody were negative controls. PD-L1 expression in tumor and immune cells was scored by cytoplasmic staining intensity: 1, weak; 2, moderate; and 3, strong (Fig. S1). PD-L1 staining intensity was divided into low (scores 1 and 2) and high (score 3) expression groups for statistical analysis. A pathologist (H.W.L.), blinded to outcomes, evaluated all sections.

2.4. Microsatellite instability (MSI) analysis

Tumor and adjacent normal tissue samples were collected separately, and genomic DNA was extracted from both using the QIAamp DNA Mini Kit (QIAGEN, Hilden, Germany). MSI analysis was performed on the extracted DNA with the U-TOP™ MSI Detection Kit, utilizing five markers (BAT25, BAT26, D5S346, D2S123, D17S250). Tumors were classified as high-frequency MSI (MSI-H) if two or more loci showed instability, low-frequency MSI (MSI-L) if one locus was unstable, and microsatellite-stable (MSS) if there was no instability.

2.5. RNA extraction, library preparation, and sequencing

Total RNA was extracted from 11 pairs of human LARC tissues before and after irradiation using TRIzol RNA Isolation Reagent (Life Technologies, Gaithersburg, MD, USA), according to the manufacturer's instructions. Total RNA was evaluated using an Agilent 2100 Bioanalyzer RNA kit (Agilent, Santa Clara, CA, USA). RNA-seq libraries were generated using an Illumina TruSeq Stranded mRNA Sample Preparation Kit (Illumina, San Diego, CA, USA), according to the manufacturer's protocol, and assessed using an Agilent 2100 Bioanalyzer DNA kit (Agilent). All libraries were quantified by quantitative real-time polymerase chain reaction (qPCR) using a CFX96 Real-Time System (Bio-Rad Laboratories, Hercules, CA, USA) and sequenced using a NextSeq500 sequencer (Illumina, San Diego, CA, USA) with a paired-end 76-bp plus a single 6-bp index read run. RNA-Seq, quality control, and mapping were performed as previously reported [19].

2.6. Bioinformatic analysis for the expression scores of PD-L1 expression-regulating genes

Raw RNA sequencing reads were subjected to quality control and trimming using FastQC, followed by alignment to GRCh38 using the STAR aligner. For between-sample comparisons, gene expression was quantified using—'quantMode' in STAR and normalized to DESeq2 using R software. PD-L1 expression-regulating genes were assessed by ssGSEA using a curated gene list (Table 1A). Paired *t*-tests were used to compare normalized PD-L1 expression and ssGSEA scores before and after CRT. Statistical analyses were performed, and plots were generated using R.

2.7. Cell culture and materials

Human CRC cell lines, DLD-1 and HCT116, were obtained from the American Type Culture Collection (ATCC; Manassas, VA, USA). Cells were cultured in RPMI 1640 medium (Welgene Inc, Gyeongsan, Korea) supplemented with 10 % fetal bovine serum (FBS; ATCC), 2 mM glutamine, 50 IU/mL penicillin, and 50 μg/mL streptomycin (Thermo Fisher Scientific, Waltham, MA, USA) and preserved in humidified 37 °C, 5 % CO_2 incubators. Anti-PD-L1 (1:2,000, #13684) and anti-β-actin (1:10,000, #A5441) were purchased from Cell Signaling Technology (Beverly, MA, USA) and Sigma Chemical Co. (St. Louis, MO, USA),

Table 1A
Primer sequences of PD-L1-related genes evaluated by quantitative PCR.

Primer name	Sequences
EGF sense	5′-CAAAACGGAGGCTGTGAACA-3′
EGF antisense	5′-CAGAAAGGCAGCCACCAAAAT-3′
EGFR sense	5′-CAGAAAGGCAGCCACCAAAT-3′
EGFR antisense	5′-TGGAGCCCTTAAAGATGCCA-3′
IL17A sense	5′-AAGGCCCCTCAGAGATCAAC-3′
IL17A antisense	5′-CCTTTCTGGGTTGTGTGGTG-3′
TNF sense	5′-TCTGGGCAGGTCTACTTTGG-3′
TNF antisense	5′-TGAGCCAGAAGAGGTTGAGG-3′
IFNG sense	5′-TCCTTTGGACCTGATCAGCT-3′
IFNG antisense	5′-CCAAAACGATGCAGAGCTGA-3′
IFGNR1 sense	5′-TCTGTGAAGAGCCGTTGTCT-3′
IFGNR1 antisense	5′-GTCTTCGGTATGCATGCCTG-3′
IFGNR2 sense	5′-GCTCACCAAAGGATGACGTC-3′
IFGNR2 antisense	5′-TGGCTTGATCTCTTCCAGGG-3′
IL4 sense	5′-GCAGTTCTACAGCCACCATG-3′
IL4 antisense	5′-GTCGAGCCGTTTCAGGAATC-3′
IL27 sense	5′-AGTGAACCTGTACCTCCTGC-3′
IL27 antisense	5′-AGGTCAGGGAAACATCAGGG-3′
JAK1 sense	5′-TGGCTGTCATGGTCCAATCT-3′
JAK1 antisense	5′-TGTTGTCAAAGTCGGTGCAG-3′
JAK2 sense	5′-CCTTTGAAGACCGGGATCCT-3′
JAK2 antisense	5′-CCCTTGCCAAGTTGCTGTAG-3′
STAT1A sense	5′-GTATGCCATCCTCGAGAGCT-3′
STAT1A antisense	5′-TAGGTGCCAAGACTGTCGAG-3′
STAT1B sense	5′-GTATGCCATCCTCGAGAGCT-3′
STAT1B antisense	5′-TAGGTGCCAAGACTGTCGAG-3′
STAT2 sense	5′-ACTCCCGCTGACTGAAATCA-3′
STAT2 antisense	5′-ATTCGGGGATAGAGGAAGCG-3′
STAT3 sense	5′-GGCGGATCATAAGGTCAGGA-3′
STAT3 antisense	5′-TTCACCGTGTTAGCCAGGAT-3′
IRF1 sense	5′-AGGGGAAAAGGAGCCAGATC-3′
IRF1 antisense	5′-CCTCGATATCTGGCAGGGAG-3′
PIK3CA sense	5′-CCTATTGTCGTGCATGTGGG-3′
PIK3CA antisense	5′-TGCCTCGACTTGCCTATTCA-3′
AKT1 sense	5′-CGACGTGGCTATTGTGAAGG-3′
AKT1 antisense	5′-TTGAGGAGGAAGTAGCGTGG-3′
RELA sense	5′-GACCAACAACAACCCCTTCC-3′
RELA antisense	5′-GCACAGCATTCAGGTCGTAG-3′
NFKB1A sense	5′-GAGCTTTTGGTGTCCTTGGG-3′
NFKB1A antisense	5′-CATCAGCCCCACACTTCAAC-3′
NFKB1 sense	5′-GGTGACAGGAGACGTGAAGA-3′
NFKB1 antisense	5′-CCATTCTCATCCTGCACAGC-3′
IKBKB sense	5′-TCCATGTCTCAGCAGCTCAA-3′
IKBKB antisense	5′-TTGCTCGCTGTACTTCTCCA-3′
MAPK3 sense	5′-TGTCAAAGCTGTCACTTCGC-3′
MAPK3 antisense	5′-CACTTCTGCTCACCACACAC-3′
MAPK1 sense	5′-TGAATGGGGATGTCAGTGCT-3′
MAPK1 antisense	5′-GTGGGGTTGCAGAAGTTCAG-3′
TLR3 sense	5′-CCCTTTGATTGCACGTGTGA-3′
TLR3 antisense	5′-GAGGTGGAGTGTTGCAAAGG-3′
TLR4 sense	5′-GGTGATTGTTGTGGTGTCCC-3′
TLR4 antisense	5′-CAAAGATACACCAGCGGCTC-3′
TLR9 sense	5′-GCTTGGTAGAGGACAGGTGT-3′
TLR9 antisense	5′-TCCCATGAGTCAAAGGCCAT-3′
MYD88 sense	5′-AGGTTCATCACTGTCTGCGA-3′
MYD88 antisense	5′-AGATACACACACACCCAGGG-3′
TRAF6 sense	5′-TACTATTAGGCTGGGCACGG-3′
TRAF6 antisense	5′-CTTCAAGTAATCCGCCAGC −3′
BRD4 sense	5′-ACAACCCTCCTGACCATGAG-3′
BRD4 antisense	5′-TCGAACACATCCTGGAGCTT-3′
KMT2A sense	5′-AGAGGAGGAGGTACAGCTGA-3′
KMT2A antisense	5′-GTAGACACCAACTGCCTCCT-3′
JUN sense	5′-AGCAGCAAAGAACTTTCCCG-3′
JUN antisense	5′-CGTCCTTCTTCTCTTGCGTG-3′
JUNB sense	5′-TGCACAAGATGAACCACGTG-3′
JUNB antisense	5′-GCTGAGGTTGGTGTAAACGG-3′
FOS sense	5′-GCTTCAACGCAGACTACGAG-3′
FOS antisense	5′-TGCGGGTGAGTGGTAGTAAG-3′
BATF sense	5′-AGCGAAGACCTGGAGAAACA-3′
BATF antisense	5′-GAGCTGCTTGATCTCCTTGC-3′
MYC sense	5′-ACTCATCCACATGCCCAAGA-3′
MYC antisense	5′-GGCTTGGACAGGTTAGGAGT-3′
HIF1A sense	5′-ATGTAATGCTCCCCTCACCC-3′
HIF1A antisense	5′-CAGGGTCAGCACTACTTCGA-3′
MTOR sense	5′-GCAGTGCTGTGAAAAGTGGA-3′
MTOR antisense	5′-CCCACTGACCTAAACCCCAT-3′
RPS6KB1 sense	5′-CTGAGGATGAGCTGGAGGAG-3′
RPS6KB1 antisense	5′GGCCCTCTGTTCACACTAGT-3′
KRAS sense	5′-TTTGGTGTCAGAGTCTCGCT-3′
KRAS antisense	5′-AATCGCTTGAACCTGGGAGA-3′
CCND1 sense	5′-GACTTTGAGGCAAGTGTGGG-3′
CCND1 antisense	5′-TTTCTTCTTGACTGGCACGC-3′
CCND2 sense	5′-AGCCAGAGGAGAAGACAACC-3′
CCND2 antisense	5′-ACCTTTCAGTCCCAGAGCTC-3′
CCND3 sense	5′-TTGCACATGATTTCCTGGCC-3′
CCND3 antisense	5′-ATCATGGATGGCGGGTACAT-3′
CMTM6 sense	5′-TCCTGAATCTTGGGCCCTTT-3′
CMTM6 sense	5′- ATTAGTCTGGGCAGGGTTCC-3′
CDK4 sense	5′-AGTGTGAGAGTCCCCAATGG-3′
CDK4 antisense	5′-CGAACTGTGCTGATGGGAAC-3′
RB1 sense	5′-TCACATTCCTCGAAGCCCTT-3′
RB1 antisense	5′-TTTGTTGGTGTTGGCACACC-3′
CDH1 sense	5′-AAGGGGTCTGTCATGGAAGG-3′
CDH1 antisense	5′-GGTGTTCACATCATCGTCCG-3′
CUL3 sense	5′-CCAAACACAGTGGTCGACAG-3′
CUL3 antisense	5′-GCCAGTTACTTGTGCACCTC-3′
CUL1 sense	5′-CAACAACGCGGTTACCAAGA-3′
CUL1 antisense	5′CACAGTATCGAGCCAGCAAC-3′
BTRC sense	5′-GGGGTGGGGAATACTGGAAA-3′
BTRC antisense	5′-GCTACAGACTGGAGGGTGTT-3′
GSK3B sense	5′-GCTCTTTGTTTGCCTGACCA-3′
GSK3B antisense	5′-CAACACCCCTTCCATCTCCT-3′
STUB1 sense	5′-GAGACATCCCCGACTACCTG-3′
STUB1 antisense	5′-TCAAAATGACCCACACGCTG-3′
COPS5 sense	5′-GACGACAACTTCTCCGCTTC-3′
COPS5 antisense	5′-TTGCTGCTGTTTCTTGTCGT-3′
CMTM6 sense	5′-TCCTGAATCTTGGGCCCTTT-3′
CMTM6 antisense	5′-ATTAGTCTGGGCAGGGTTCC-3′
CMTM4 sense	5′-TAAAATGGTGAGAGGCCGGT-3′
CMTM4 antisense	5′-GCTCGCACTGATTCTGGAAG-3′
SIGMAR1 sense	5′-AACCCAGCAGCAATTTGAGG-3′
SIGMAR1 antisense	5′-TATGGTGAGGACAGGGGAGA-3′
TREX1 sense	5′-TGCCTTTGTGGATAGCA-3′
TREX1 antisense	5′-TATAGCTCTTCCTTGGGCCG-3′
CD274 sense	5′-ATTCCGGCAGTGTACCTTGA-3′
CD274 antisense	5′-CAAGGGTTCAAGCACAACGA-3′

respectively.

2.8. Irradiation

To estimate the response to radiation, HCT116 (0.07×10^6 cells/well) and DLD-1 (0.1×10^6 cells/well) cells were plated in six-well plates and incubated at 37 °C and 5 % CO_2 under humidified conditions. The cells were irradiated with 8 Gy X-rays radiation in one fraction (6 mega-voltage; dose rate: 200 cGy/s) using a linear accelerator (VitalBeam; Varian, USA). Next, to eliminate the effects of radiation, the culture medium was replaced with fresh medium. For fractionated irradiation, we applied 1.8 Gy in 10 fractions, the same daily dose of conventional fractionated radiotherapy, which is currently the main treatment for patients with LARC. After each radiation exposure, the medium was changed to mitigate side effects, and the cells were harvested 0 and 3 days after irradiation.

2.9. XTT assay

Cell viability was assessed using a 2,3-bis (2-methoxy-4-nitro-5-sulphonyl)- 2H-tetrazolium-5-carboxanilide (XTT) assay (Welgene Inc, Gyeongsan, Korea). DLD-1 and HCT116 cells were adjusted to 3×10^3 cells per well in 200 μL of medium and seeded into 96-well plates. Cells were pretreated with various concentrations of radiation for 72 h and then incubated in a 0.5 mg/mL XTT solution for 2 h at 37 °C in the dark. The optical density (OD) was measured at 450 nm using a microplate reader (BMG Labtech, Ortenberg, Germany). The experiment was

performed in triplicate.

2.10. Clonogenic assay

DLD-1 and HCT116 cells were seeded into 6-well plates at 2000 cells / well in final volume of 2 mL medium. The cells were pretreated with various concentrations of radiation. After radiation exposure, the medium was changed to mitigate side effects. Cells were cultured to allow single cells to form colonies and the medium (RPMI, 10 % FBS) was changed every 2 days. The medium was then aspirated, and the dishes were washed once with PBS, fixed with 100 % methanol for 30 min, and stained with a filtered solution of 0.5 % (w/v) crystal violet (Sigma, St. Louis, MO, USA) for 30 min. The wells were washed twice with PBS, dried at room temperature, and the defined colonies were manually scored under an inverted microscope and counted using ImageJ software (National Institutes of Health, Bethesda, Maryland, USA).

2.11. RNA isolation and quantitative RT-PCR

Total RNA was extracted from CRC cells using TRIzol reagent (Molecular Research Center, Inc., Cincinnati, OH, USA), quantified with a NanoDrop1000 (Thermo Fisher Scientific), and reverse transcribed into cDNA using ReverTra Ace® qPCR RT Master Mix (TOYOBO, Osaka, Japan). qPCR was performed on a LightCycler 480 (Roche Diagnostics, Mannheim, Germany) using specific primers (Table 1) and SYBR Green Premix (TOYOBO). β-Actin was used for normalization, and a no-template sample served as a negative control. Data were analyzed using the $2^{-\Delta\Delta Cq}$ method [21]. All experiments were conducted in triplicate. Primer sequences for PD-L1 and immune checkpoint genes are listed in Table 1A and 1B.

Table 1B
Primer sequences of immune checkpoint genes evaluated by quantitative PCR.

Primer name	Sequences
ADORA2A sense	5′-TGGAGTGACAAAGCTGGGAT-3′
ADORA2A antisense	5′-TCTGGCACTGCTCTGTTACA-3′
VSIR sense	5′-AGGATTTTGGGGTGCTGAGA-3′
VSIR antisense	5′-TGGCATCTGTAGCTGGTGAA-3′
CD276 sense	5′-GCTTTCGTGTGCTGGAGAAA-3′
CD276 antisense	5′-CCTGCATTCTCCTCCTCACA-3′
CD80 sense	5′-CATTGTGATCCTGGCTCTGC-3′
CD80 antisense	5′-TAACGTCACTTCAGCCAGGT-3′
CD86 sense	5′-GCAGGACCAGGAAAACTTGG-3′
CD86 antisense	5′-CGAATCAAAACTTGTGCGGC-3′
LGALS9 sense	5′-GCTCCCATTACCCAGACAGT −3′
LGALS9 antisense	5′-TGGCGGGAGTAGAGAACATC −3′
TNFSF4 sense	5′-AATGTGGGAAATGCAGCCAG-3′
TNFSF4 antisense	5′-AAGTGCAGGCAGATGTAGGT-3′
CD40 sense	5′-CCCATCCAGTCTCCCAACTT-3′
CD40 antisense	5′-CCACCACCACCAAACTTCTG-3′
ICOSLG sense	5′-TCAGCCAGGACCTGTTACAG-3′
ICOSLG antisense	5′-AGTCTGGGTCTGAGAAGTGC-3′
TNFRSF14 sense	5′-TGCAGTCCAGGTTATCGTGT-3′
TNFRSF14 antisense	5′-CATTTGGCACTGCAGACACT-3′
HLA-A sense	5′-GGGACTGAGAGGCAAGAGTT-3′
HLA-A antisense	5′-ACACGAACACAGACACATGC-3′
HLA-B sense	5′-ATGCAGGATTTCTTCACGCC-3′
HLA-B antisense	5′-TAACAGGGACGCAGACACAT-3′
HLA-C sense	5′-GTAAAGCCTGAGACAGCTGC-3′
HLA-C antisense	5′-GGAACGCAGACACATTCAGG-3′
TNFSF18 sense	5′-TAGTTCACCAGCACACCACT-3′
TNFSF18 antisense	5′-TGCCCTGAGAAATCACCAGT-3′
TNFSF9 sense	5′-CATGAGTCAATGCAGCCTCC-3′
TNFSF9 antisense	5′-ATAGCAATACCGTCTCCGCA-3′
PVR sense	5′-GATATCTGGCTCCGAGTGCT-3′
PVR antisense	5′-AGCTGGACCTTCTGAACCTC-3′
NECTIN2 sense	5′-CTGTCCTATAGCAGCCCCTC-3′
NECTIN2 antisense	5′-CAGCTCACACATACATGGCC-3′
β-actin sense	5′-CAGCCATGTACGTTGCTATCCAGG-3′
β-actin antisense	5′-AGGTCCAGACGCAGGATGGCATG-3′

2.12. Western blotting analysis

The cells were resuspended in RIPA lysis buffer (50 mM Tris–HCl pH 7.4, 150 mM NaCl, 0.1 % SDS, 0.25 % sodium deoxycholate, 1 mM EDTA, 1 mM EGTA, 0.1 % NP-40, plus proteinase inhibitors) and incubated on ice for 10 min. Total protein was quantified using the Bradford assay. Approximately 50 μg of each protein extract was separated on 8 % sodium dodecyl sulfate polyacrylamide gel electrophoresis and transferred to cellulose membranes (Whatman, Thermo Fisher Scientific, Inc.). Nonspecific binding was blocked with 5 % skim milk for 1 h, after which the membranes were incubated with primary antibodies overnight. Specific proteins were detected using an ECL Western blotting kit (Millipore, Billerica, MA, USA) according to the manufacturer's instructions.

2.13. Evaluation of membranous PD-L1 expression

Protein extractions of membrane fractions were performed using Mem-PER Extraction kit (Thermo Fisher Scientific Inc. Waltham, MA, USA), according to manufacturer's recommendation. Cells were harvested and washed with Mem-PER reagent A, the supernatant was discarded, cells were resuspended in reagent B and centrifuged to collect cytoplasmic proteins, then reagent C was added to the pellet, incubated, and centrifuged to isolate membrane proteins. The isolated membrane protein fraction was directly analyzed using SDS-PAGE and western blotting.

2.14. Statistical analyses

Differences in clinicopathological features between responder and non-responders before and after CRT were analyzed using Fisher's exact tests for categorical variables. Differences in *CD274* mRNA expression between groups before and after CRT were statistically analyzed using a paired *t*-test. PD-L1 expression and immune cell reaction before and after CRT were evaluated using the standard McNemar's test. To predict tumor response, relative risk was calculated for the evaluation of pre-CRT immuno-oncological markers. Statistical analyses were performed using IBM SPSS Statistics for Windows version 25.0 (IBM Corp., Armonk, NY, USA). Statistical significance was set at $p < 0.05$.

3. Results

3.1. Clinicopathological characteristics of patients

The clinicopathological characteristics of all patients are presented in Table 2. Regarding TRG, 9 (37.5 %) patients were categorized as responders and 15 (62.5 %) as non-responders. The demographic characteristics were comparable between the two cohorts. Tumor stage, which was classified as early stages (T0, 1, 2) in more patients in the responder group and advanced stages in more patients in the non-responder group (p=0.033), was the only demographic characteristic that differed between the two groups (Table 2).

3.2. PD-L1 expression, immune cell reaction, and MSI according to TRG

No significant differences were observed between the TRG categories in pre- and post-CRT PD-L1 expression in tumors and tumor-infiltrating immune cells by IHC, pre- and post-CRT immune cell reactions, or pre- and post-CRT MSI status (Table 3). However, patients with MSI-H status were classified as responders in both pre- and post-CRT tumor tissues, and there were no patients with pre-CRT MSI-H status in the non-responder group. In 1 patient of the responder group, MSI status changed from MSI-H (instability in D5S346 and D17S250) to MSS; however, there was also 1 patient who was still MSI-H after CRT and 1 patient whose MSI status changed from MSI-L to MSI-H after CRT (Table 3, Fig. S2).

Table 2
Characteristics of patients.

	All patients (N = 24)	Responder (N = 9)	Non-responder (N = 15)	P-value
Age (years), n (%)				0.657
≤60	8 (33.3)	2 (22.2)	6 (40.0)	
>60	16 (66.7)	7 (77.8)	9 (60.0)	
Sex, n (%)				1.000
Male	19 (79.2)	7 (77.8)	12 (80.0)	
Female	5 (20.8)	2 (22.2)	3 (20.0)	
BMI (kg/m^2), n (%)				1.000
≤23	9 (37.5)	3 (33.3)	6 (40.0)	
>23	15 (62.5)	6 (66.7)	9 (60.0)	
Preoperative CEA level (ng/mL)				1.000
≤5	19 (79.2)	7 (77.8)	12 (80.0)	
>5	5 (20.8)	2 (22.2)	3 (20.0)	
Tumor stage, n (%)				0.033
T 0, 1, 2	14 (58.3)	8 (88.9)	6 (40.0)	
T 3	10 (41.7)	1 (11.1)	9 (60.0)	
Nodal stage, n (%)				1.000
N0	18 (75.0)	7 (77.8)	11 (73.3)	
N1,2	6 (25.0)	2 (22.2)	4 (26.7)	
Histology				0.130
Well and moderate	22 (91.7)	7 (77.8)	15 (100)	
Poor	2 (8.3)	2 (22.2)	0 (0)	
Tumor budding	2 (8.3)	0 (0)	2 (13.3)	0.511
Lymphovascular invasion, n (%)	0 (0)	0 (0)	0 (0)	1.000
Perineural invasion	3 (12.5)	0 (0)	3 (20.0)	0.266
Extranodal extension, n (%)	2 (8.3)	0 (0)	2 (13.3)	0.511
KRAS mutation, n (%)	7 (29.2)	3 (33.3)	4 (26.7)	0.657
BRAF mutation, n (%)	2 (8.3)	1 (11.1)	1 (6.7)	1.000

BMI, body mass index; CEA, carcinoembryonic antigen.

Table 3
PD-L1 expression, intra-tumoral immune cell reaction, and MSI status according to tumor regression grade.

	Responder (N = 9)	Non-responder (N = 15)	P-value
Pre-CRT PD-L1 expression on tumor cells, n (%)			0.615
Low	7 (77.8)	13 (86.7)	
High	2 (22.2)	2 (13.3)	
Pre-CRT PD-L1 expression on immune cells, n (%)			0.403
Low	4 (44.4)	10 (66.7)	
High	5 (55.6)	5 (33.3)	
Pre-CRT intra-tumoral immune cell reaction, n (%)			0.403
No and mild	4 (44.4)	10 (66.7)	
Moderate and severe	5 (55.6)	5 (33.3)	
Pre-CRT MSI status, n (%)			0.130
MSI-high	2 (22.2)	0 (0)	
MSS-low and MSS	7 (77.8)	15 (100.0)	
Post-CRT PD-L1 expression on tumor, n (%)			0.319
Low	4 (80.0)	7 (46.7)	
High	1 (20.0)	8 (53.3)	
Post-CRT PD-L1 expression on immune cell, n (%)			0.347
Low	3 (60.0)	5 (33.3)	
High	2 (40.0)	10 (66.7)	
Post-CRT *peri*-tumoral immune cell reaction, n (%)			0.266
No and mild	9 (100.0)	12 (80.0)	
Moderate and severe	0 (0)	3 (20.0)	
Post-CRT MSI status, n (%)			0.130
MSI high	2 (22.2)	0 (0)	
MSS-low and MSS	7 (77.8)	15 (100.0)	

PD-L1, programmed death-ligand 1; CRT, chemoradiation therapy; MSI, microsatellite instability; MSS, microsatellite stable.
P-value was the result of Fisher's exact test.

3.3. CRT induces PD-L1 upregulation in the non-responder group

PD-L1 expression was significantly increased after CRT in 8 (47.1 %) of the 17 patients with low PD-L1 expression (McNemar's test, p = 0.058) (Table 4). Interestingly, PD-L1 staining intensity increased after CRT in 7 (53.9 %) of 13 patients with low PD-L1 expression in the non-responder group (McNemar's test, p = 0.034). Tumor-infiltrating immune cell PD-L1 expression showed no significant difference between the responder and non-responder groups before and after CRT. Next, we determined whether CRT regulates PD-L1 mRNA expression in LARC tissues. *CD274* (gene symbol of PD-L1) was upregulated in 7 of the 8 patients with CRC (p = 0.041) in the non-responder group.

3.4. RT induces PD-L1 upregulation in relatively radioresistant human CRC cells

To validate the results observed in the LARC tissues, we used two human CRC cell lines with differential radiosensitivity [22] to demonstrate the effect of RT on PD-L1 expression. After single fractioned irradiation, cellular viability was evaluated. The growth-inhibitory effect was more pronounced in HCT116 than in DLD-1 cells (Fig. 1B). Moreover, a clonogenic survival analysis revealed that DLD-1 was more resistant to radiation than HCT116 (Fig. 1C and D). Next, we investigated the effect of the fractionated irradiation on PD-L1 expression in human CRC cells. The results showed that, compared to that in HCT116 cells, PD-L1 expression increased by 4.13- and 8.04-fold in radiosensitive HCT116 cells and by 8.49- and 25.13-fold in radioresistance DLD-1 cells, respectively, on days 0 and 3 (Fig. 1E; day 0, p=0.051; day 3, p=0.036). The two cell lines were irradiated to examine the differences in PD-L1 expression. We found that, compared to HCT116 cells, RT upregulated PD-L1 mRNA expression (Fig. 1F) and induced the upregulation of membranous PD-L1 (Fig. 1G) in relatively radioresistant DLD-1.

Table 4
PD-L1 expression and intratumoral immune cell reaction before and after CRT.

After (N = 20)Before (N = 24)	Lown (%)	Highn (%)	P-value	*Missing sample
PD-L1 expression in tumor cells in all patients			0.058	
Low (weak and moderate)	9 (52.9)	8 (47.1)		3
High (strong)	2 (66.7)	1 (33.3)		1
PD-L1 expression in tumor cells in responders			1.000	
Low	3 (75.0)	1 (25.0)		3
High	1 (100.0)	0 (0.0)		1
PD-L1 expression in tumor cells in non-responders			0.034	
Low	6 (46.1)	7 (53.9)		
High	1 (50.0)	1 (50.0)		
PD-L1 expression in immune cells in all patients			0.248	2
Low (weak and moderate)	4 (33.3)	8 (66.7)		2
High (strong)	4 (50.0)	4 (50.0)		
PD-L1 expression in immune cells in responders			0.564	
Low	1 (50.0)	1 (50.0)		2
High	2 (66.7)	1 (33.3)		2
PD-L1 expression in immune cells in non-responders				
Low	3 (30.0)	7 (70.0)	0.096	
High	2 (40.0)	3 (60.0)		

PD-L1, programmed death-ligand 1.
P-value was the result of McNemar test.*Missing samples are due to complete response after CRT.

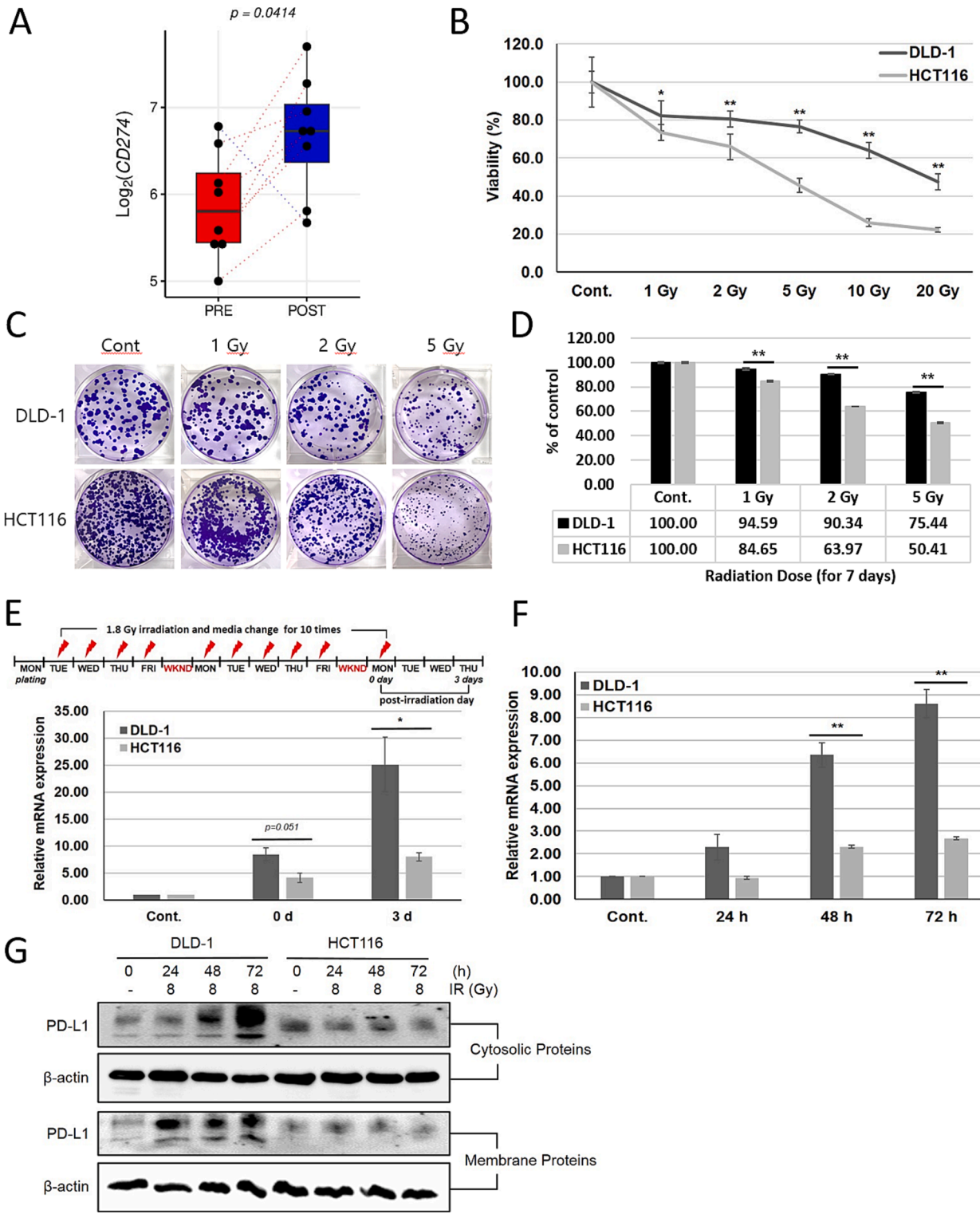

Fig. 1. Radiotherapy (RT) induces PD-L1 upregulation in relatively radioresistant human locally advanced rectal cancer (LARC) tissues and colorectal cancer (CRC) cells. (A) Comparison of *CD274* mRNA expression between LARC tissues before and after neoadjuvant chemoradiotherapy (n = 8). (B) Cell proliferation assay. Cells were irradiated with the indicated Gys. After 72 h, the XTT assay was performed. The growth of cells without radiation was considered to be 100 %, * $p<0.05$, ** $p<0.005$ (DLD-1 vs HCT116). (C) Clonogenic survival assay. Cells were irradiated with the indicated Gys. The growth of cells without radiation was considered to be 100 %. (D) Graphical representation of defined colony from three random images (** $p<0.005$, DLD-1 vs HCT116). (E) Relative *CD274* mRNA expression in CRC cells. Cells were exposed to a total radiation dose of 1.8 Gy 10 times, then the culture medium was replaced, and cells were harvested on days 0 and 3 following radiation. mRNA expression was measured using real-time PCR (normalized to the corresponding β-actin mRNAs), * $p<0.05$ (DLD-1 vs HCT116). (F) Relative *CD274* mRNA expression in CRC cells. Cells were treated with 8 Gy radiation for the indicated periods. mRNA levels were measured using real-time PCR (normalized to the corresponding β-actin mRNAs), ** $p<0.005$ (DLD-1 vs HCT116). (G) Cells were treated with 8 Gy radiation for the indicated periods. Cytosolic and membrane proteins and protein expression levels of PD-L1 were separated. Blots/gels are presented in Fig. S3. The expression level of β-actin was used as a protein loading control.

3.5. CRT modulates PD-L1 expression-regulating genes in human LARC tissues and CRC cells

Various genes are involved in cancer cell PD-L1 expression [23]. We investigated whether CRT-induced increase of PD-L1 expression in LARC tissues was accompanied by changes in PD-L1 expression-regulating genes. The expression scores of PD-L1 expression-regulating genes were elevated following CRT (Fig. 2A). In seven of eight patients who exhibited elevated PD-L1 levels following CRT, the scores of PD-L1-regulating genes demonstrated a concurrent increase after CRT (Fig. 2A, $p = 0.0451$). A detailed analysis of each gene has been included in Fig. S4. Next, using two CRC cell lines (DLD-1 (radioresistant) and HCT116 (radiosensitive) cells), we determined the factors regulated by RT that drive PD-L1 expression. Similar to the change in PD-L1 expression observed in CRC tissue, we found that RT upregulated PD-L1 expression-regulating genes prominently in radioresistant DLD-1 cells (Fig. 2B, Fig. S5). For example, *AKT*, *BATF*, *CMTM4*, *EGFR*, *IFNGR1*, *IRF1*, *JAK1*, *JAK2*, *KMT2A*, *KRAS*, *MAPK3*, *NFKB1A*, *PIK3CA*, *RELA* and *TREX1* were upregulated in radioresistant DLD-1 cells at 48 and 72 h. In addition, *BTRC*, *CDH1*, *CUL1*, *CLU3*, *JUNB*, and, *MTOR* were upregulated in radioresistant DLD-1 cells at 72 h. *IFNG*, *IKBKB*, *STAT2*, *STAT3*, and *TRAF6* were upregulated in radioresistant DLD-1 cells at 72 h. Notably, the *IFNGR2* gene was significantly upregulated in DLD-1 cells than in HCT116 cells at every time point. In contrast, *BRD4, CCND1, CCND2, CCND3, CDK4, CMTM6, COPS5, EGF, FOS, GSK3B, HIF1A, IL17A, IL27, IL4, JUN, MAPK1, MYC, MYD88, NFKB1, RB1, RPS6KB1, SIGMAR1, STAT1A, STAT1B, STUB1, TLR3, TLR4, TLR9* and *TNF* were not differentially expressed between the two cell lines and were not upregulated in radiation-resistant DLD-1 cells (Fig. 2B, Fig. S5).

3.6. CRT modulates various immune checkpoints in human LARC tissues and CRC cells

In addition to PD-L1, various immune checkpoints have recently been reported as targets for immunotherapy [24,25]. Therefore, we investigated whether CRT could regulate other immune checkpoints. CRT significantly upregulated *HLA-A* ($p = 0.036$) and *CD86* ($p = 0.016$) and downregulated *PVR* (gene symbol of CD155) in the non-responder group with increased PD-L1 expression (Fig. 3A). A trend towards increased *HLA-C* ($p = 0.058$) and *LGALS9* (gene symbol of Galectin-9, $p = 0.061$) expression was observed. However, differential expression of *HLA-B*, *CD276* (gene symbol of B7-H3), *CD40*, *TNFSF4* (OX40L), *TNFSF9* (gene symbol of 4-1BBL), *ICOSLG* (gene symbol of B7RP1), *CD80*, *ADORA2A* (gene symbol of A2aR), *TNFSF18* (a gene signature of GITRL), and *TNFRSF14* (gene symbol of HVEM) between the two groups was not significant. Next, two CRC cell lines were used to validate whether RT regulates immune checkpoints in human CRC cells. At every time point, *NECTIN2* (gene symbol of CD112) expression was significantly higher in DLD-1 than in HCT116 cells (Fig. 3B, Fig. S6). Similar to the change in PD-L1 expression, RT significantly increased the expression of *CD276*, *HLA-A*, *HLA-B*, *ICOSLG,* and *VSIR* (gene symbol of VISTA) at 48 and 72 h in the relatively radioresistant DLD-1 cells compared with the relatively radiosensitive HCT116 cells (Fig. 3B, Fig. S6). We also found that *ADORA2A*, *HLA-C*, *LGALS9,* and *TNFSF9* increased significantly in radioresistant DLD-1 cells at 72 h. In contrast, in radiosensitive HCT116 cells, the RT-induced increase in *CD40*, *CD80*, and *TNFSF18* expression was significantly higher than that in radioresistant DLD-1 cells. However, *PVR* which was downregulated in RNA-seq, was upregulated in CRC cells. Similarly, *CD86,* which was upregulated according to RNA-seq data, was downregulated in CRC cells.

4. Discussion

CRT delivers ionizing radiation to target malignant cells, causing DNA damage and immunogenic cell death, which boosts immune response by releasing danger-associated molecular patterns [9,26]. Cell irradiation increases neoantigen levels, activates major histocompatibility complex molecules, and activates tumor-infiltrating lymphocytes, which affect the response to immune checkpoint inhibitors (ICIs) [27,28]. Chiang et al. found that neoadjuvant CRT triggers PD-L1 upregulation in tumor cells of patients with locally advanced rectal cancer, suggesting that radiation-induced IFN-γ production increases PD-L1 expression [29]. In contrast to Chiang et al. finding that radiation upregulated PD-L1 protein in cell culture, Saigusa et al. found that irradiation decreased PD-L1 mRNA in colorectal cancer cell lines [30]. However, high PD-L1 membrane expression is linked to better immunotherapy responses [31]. In our study, 53.9 % of non-responders showed increased PD-L1 expression after radiotherapy, along with upregulation of ICI targets in CRC cells. Therefore, combining neoadjuvant CRT with ICIs could benefit non-responders to CRT.

Since radiosensitivity can be assessed by colony formation [32], we performed a clonogenic assay on two colon cancer cell lines, HCT116 and DLD-1. Our study revealed increased PD-L1 expression after radiotherapy (RT), especially in radioresistant DLD-1 cells, through both RT-qPCR and immunoblotting. Recently, regulatory pathways related to PD-L1 expression were identified for various cancers [33]. Therefore, we investigated regulatory factors in human LARC tissue and CRC cell lines, finding that CRT and RT altered PD-L1 expression, particularly in RT-

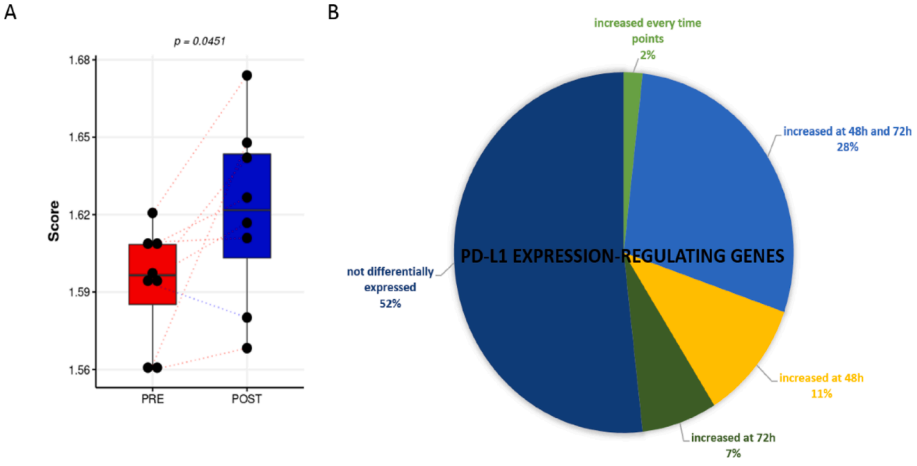

Fig. 2. RT regulates PD-L1 expression-regulating genes in human LARC tissues and CRC cells. (A) Comparison of the PD-L1 expression-regulating gene scores between LARC tissues before and after neoadjuvant chemoradiotherapy. (B) Relative PD-L1-regulating gene expression in CRC cells. Cells were treated with 8 Gy radiation for 24, 48, and 72 h. % indicates the percentage of genes (of the total 56 genes) that increased in DLD-1 compared to HCT116 cells.

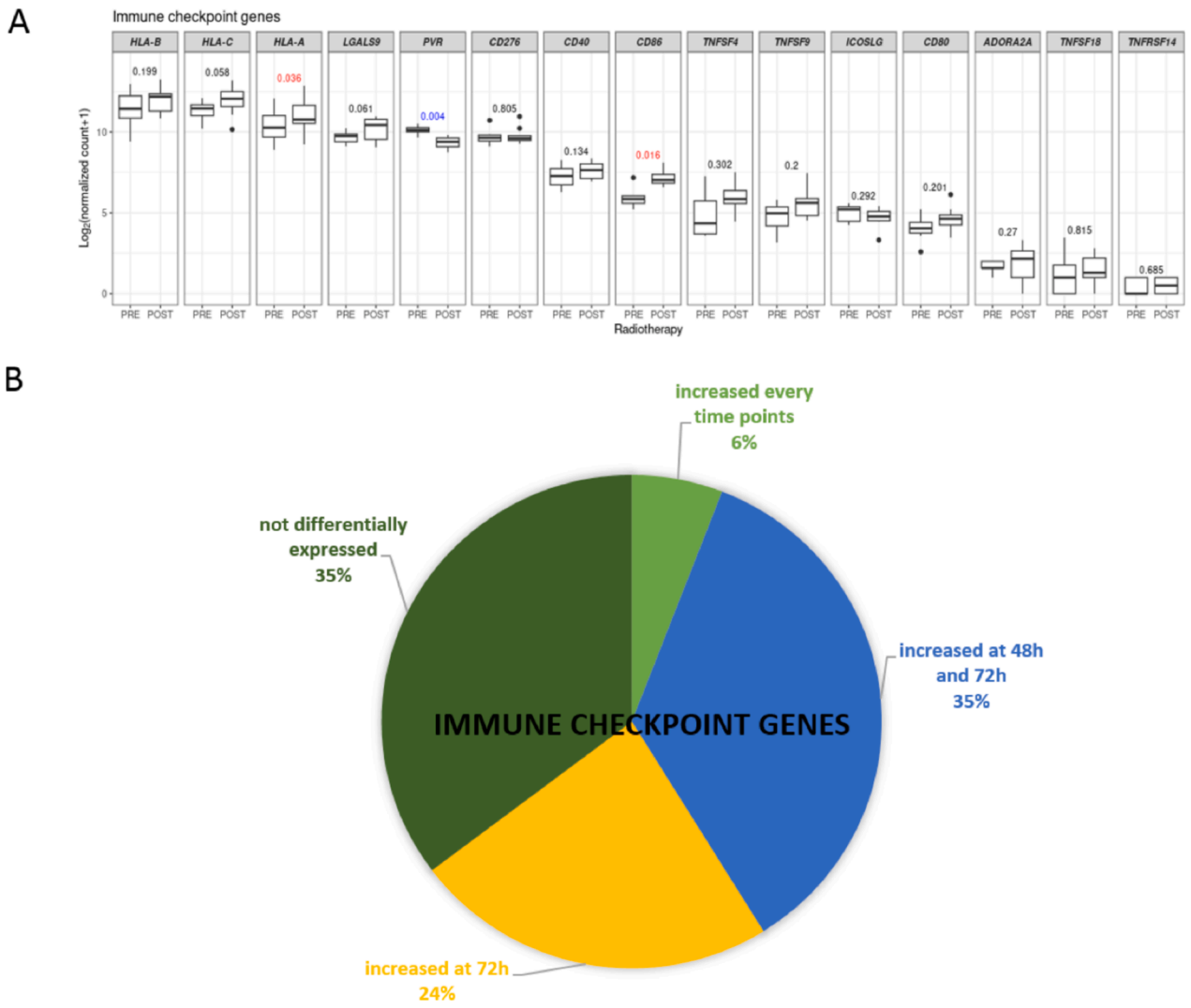

Fig. 3. RT regulates immune checkpoint genes in human LARC tissues and CRC cells. (A) Comparison of the expression levels of immune checkpoint genes in a non-responder group of LARC before and after chemoradiation therapy (CRT). (B) Relative mRNA expression levels of immune checkpoint genes in CRC cells. Cells were treated with 8 Gy radiation for 24, 48, and 72 h. The number % indicates the percentage of the number of genes increased in DLD-1 compared to HCT116 out of the total 17 genes.

resistant groups, indicating that RT upregulates PD-L1 by regulating associated genes.

RT-induced antitumor immune responses can be inhibited by checkpoint molecules [34,35]. Combining radiation with PD-1/PD-L1 blockade has shown synergistic tumor growth inhibition and the "abscopal effect" in animal models [7,9], with clinical support in bladder, lung, and esophageal cancers [8,15,36]. Our study found increased PD-L1 expression in non-responder tumor cells. Thus, combining CRT with ICIs, starting with immunomodulation, may be an effective treatment for locally advanced rectal cancer [37].

CD86, expressed on antigen-presenting cells (APCs), plays a crucial role in immune responses by promoting T-cell activation via interaction with *CD28*, while interaction with CTLA-4 inhibits T cells and aids cancer immune evasion [38]. Our study found that CRT increased *CD86* levels in radioresistant LARC tissues and RT increased *CD86* in radiosensitive HCT116 cells. This suggests that RT may activate T-cells through increased *CD86*, although this effect can vary with cancer type and microenvironment. *HLA-A*, *HLA-B* and *HLA-C* encode MHC I, which present protein fragments to CD8+ T cells but also promote self-tolerance by inhibiting NK cells [39]. Moreover, *HLA-A* is highly expressed in colorectal cancer but not linked to prognosis, whereas its downregulation is associated with better outcomes [40]. Our study found that CRT increased HLA-A in radioresistant LARC tissues and RT increased HLA-A in radioresistant DLD-1 cells. These results suggest that combining CRT with an HLA-A antagonist could enhance NK cell anti-cancer activity. *PVR*, an immune checkpoint gene, was decreased by CRT in LARC tissues but increased in radioresistant DLD-1 cells. PVR, highly expressed in several cancers, modulates immunity by interacting with immune cell receptors and suppressing T-cell immunity via TIGIT binding, associated with poor prognosis [41]. Despite *PVR* knockdown inducing apoptosis in non small cell lung cancer [42], our study found increased PVR in radioresistant DLD-1 cells, differing from LARC tissues. These findings highlight the need for further research on CRT effects on PVR and potential PVR-targeting immunotherapies in colorectal cancer. Overall, CRT and RT alter various immune checkpoints, suggesting that combining neoadjuvant CRT with specific immune checkpoint inhibitors could enhance antitumor responses.

Approximately 15 % of colorectal carcinomas exhibit high microsatellite instability (MSI-H), linked to higher tumor-infiltrated lymphocytes, better prognosis, right-sided location, and poor differentiation [43]. MSI cancers may be more radiosensitive due to the role of MMR proteins in DNA repair, though findings are mixed [44–48]. In our study, all MSI-H patients (two before CRT, two after) were responders, while no non-responders had MSI-H status. This suggests MSI-H may be a

predictive biomarker for CRT response in locally advanced rectal cancer, though further validation is needed due to the small sample size.

Our study has limitations, including a small sample size, no in vitro investigation of different radiation doses and fractionations, and no exploration of various immune cell populations or in vivo models. We used only one radiation dose (8 Gy in a single fraction) to show increased PD-L1 expression in CRC cells. Despite these limitations, the study demonstrated that CRT induces higher PD-L1 expression in radioresistant cancer cells, supporting a treatment strategy combining CRT with PD-L1 blockade to overcome radioresistance in rectal adenocarcinoma.

5. Conclusions

This study examined how neoadjuvant CRT affects PD-L1 expression in LARC and its clinical implications. CRT increased PD-L1 expression in non-responders, while high microsatellite instability was linked to better CRT response. CRT also upregulated PD-L1 and related immune checkpoint genes in CRC cells. Additionally, conventional radiation may enhance the effectiveness of immune checkpoint inhibitors (ICIs). Overall, combining radiotherapy with PD-L1 blockade could be a promising strategy to address radioresistance in CRC.

CRediT authorship contribution statement

Sung Uk Bae: Conceptualization, Methodology, Investigation, Resources, Data curation, Writing – original draft, Supervision, Project administration, Funding acquisition. **Hye Won Lee:** Conceptualization, Validation, Investigation, Resources, Data curation, Writing – original draft, Visualization, Funding acquisition. **Jee Young Park:** Validation, Formal analysis, Investigation, Data curation, Writing – original draft, Writing – review & editing, Visualization. **Incheol Seo:** Conceptualization, Methodology, Software, Formal analysis, Investigation, Resources, Data curation, Writing – original draft, Writing – review & editing, Visualization, Funding acquisition. **Jae-Min Cho:** Writing – original draft, Visualization. **Jin Young Kim:** Formal analysis, Investigation, Resources. **Ju Yup Lee:** Formal analysis, Investigation, Resources. **Yoo Jin Lee:** Formal analysis, Resources. **Seong Kyu Baek:** Formal analysis, Resources. **Nam Kyu Kim:** Formal analysis, Investigation, Resources, Supervision. **Sang Jun Byun:** Conceptualization, Methodology, Validation, Writing – original draft, Funding acquisition. **Shin Kim:** Conceptualization, Methodology, Validation, Investigation, Resources, Data curation, Writing – original draft, Writing – review & editing, Supervision, Project administration, Funding acquisition.

Declaration of competing interest

The authors declare that they have no known competing financial interests or personal relationships that could have appeared to influence the work reported in this paper.

Acknowledgements

We would like to thank all the members of our research group for their enthusiastic participation in this study.

Funding

This work was supported by the National Research Foundation of Korea (grant funded by the Korea Government Ministry of Science, ICT and Future Planning; grant no. RS-2024-00439078, RS-2023-00249115, 2022R1C1C1012908, 2021R1F1A1064310, 2020R1G1A1101226, and 2018R1C1B508574413).

Ethics approval and consent to participate

The present study was approved by the Institutional Review Board of Keimyung University and Dongsan Medical Center (IRB No. 2016-08-020) and performed in accordance with the principles of the Declaration of Helsinki. All patients provided written informed consent to allow the use of their tissues.

Consent for publication

All authors reviewed the manuscript and consented for publication.

Appendix A. Supplementary data

Supplementary data to this article can be found online at https://doi.org/10.1016/j.ctro.2024.100906.

Data availability

The raw RNA sequencing data were deposited into the Gene Expression Omnibus database under accession number GSE233517 and are available at the following URL: https://www.ncbi.nlm.nih.gov/geo/query/acc.cgi?acc=GSE233517.

References

[1] Minsky BD, et al. The efficacy of preoperative 5-fluorouracil, high-dose leucovorin, and sequential radiation therapy for unresectable rectal cancer. Cancer 1993;71(11):3486–92.
[2] van Gijn W, et al. Preoperative radiotherapy combined with total mesorectal excision for resectable rectal cancer: 12-year follow-up of the multicentre, randomised controlled TME trial. Lancet Oncol 2011;12(6):575–82.
[3] Lim DR, et al. Long-term oncological outcomes of robotic versus laparoscopic total mesorectal excision of mid-low rectal cancer following neoadjuvant chemoradiation therapy. Surg Endosc 2017;31(4):1728–37.
[4] Kim NK, Kim MS, Al-Asari SF. Update and debate issues in surgical treatment of middle and low rectal cancer. J Korean Soc Coloproctol 2012;28(5):230–40.
[5] Carvalho HA, Villar RC. Radiotherapy and immune response: the systemic effects of a local treatment. Clinics (Sao Paulo) 2018;73(suppl 1):e557s.
[6] Khanna KK, Jackson SP. DNA double-strand breaks: signaling, repair and the cancer connection. Nat Genet 2001;27(3):247–54.
[7] Demaria S, et al. Ionizing radiation inhibition of distant untreated tumors (abscopal effect) is immune mediated. Int J Radiat Oncol Biol Phys 2004;58(3):862–70.
[8] Vatner RE, et al. Combinations of immunotherapy and radiation in cancer therapy. Front Oncol 2014;4:325.
[9] Wennerberg E, et al. Immune recognition of irradiated cancer cells. Immunol Rev 2017;280(1):220–30.
[10] Topalian SL, Drake CG, Pardoll DM. Immune checkpoint blockade: a common denominator approach to cancer therapy. Cancer Cell 2015;27(4):450–61.
[11] Wu M, et al. Improvement of the anticancer efficacy of PD-1/PD-L1 blockade via combination therapy and PD-L1 regulation. J Hematol Oncol 2022;15(1):24.
[12] Patel SP, Kurzrock R. PD-L1 expression as a predictive biomarker in cancer immunotherapy. Mol Cancer Ther 2015;14(4):847–56.
[13] Deng L, et al. Irradiation and anti-PD-L1 treatment synergistically promote antitumor immunity in mice. J Clin Invest 2014;124(2):687–95.
[14] Gong X, et al. Combined radiotherapy and anti-PD-L1 antibody synergistically enhances antitumor effect in non-small cell lung cancer. J Thorac Oncol 2017;12(7):1085–97.
[15] Lim SH, et al. Changes in tumour expression of programmed death-ligand 1 after neoadjuvant concurrent chemoradiotherapy in patients with squamous oesophageal cancer. Eur J Cancer 2016;52:1–9.
[16] Hecht M, et al. PD-L1 is upregulated by radiochemotherapy in rectal adenocarcinoma patients and associated with a favourable prognosis. Eur J Cancer 2016;65:52–60.
[17] Chiang SF, et al. Upregulation of tumor PD-L1 by neoadjuvant chemoradiotherapy (neoCRT) confers improved survival in patients with lymph node metastasis of locally advanced rectal cancers. Cancer Immunol Immunother 2019;68(2):283–96.
[18] Sun G, et al. Treatment of patients with cancer using PD1/PDL1 antibodies: Adverse effects and management strategies (Review). Int J Oncol 2022;60(6).
[19] Seo I, et al. Neoadjuvant chemoradiation alters biomarkers of anticancer immunotherapy responses in locally advanced rectal cancer. J Immunother Cancer 2021;9(3).
[20] Mandard AM, et al. Pathologic assessment of tumor regression after preoperative chemoradiotherapy of esophageal carcinoma. Clinicopathol Correlations Cancer 1994;73(11):2680–6.
[21] Schmittgen TD, Livak KJ. Analyzing real-time PCR data by the comparative C(T) method. Nat Protoc 2008;3(6):1101–8.

[22] Pan H, et al. Radiation engenders converse migration and invasion in colorectal cancer cells through opposite modulation of ANXA2/AKT/GSK3beta pathway. Am J Cancer Res 2021;11(1):61–78.
[23] Shi Y. Regulatory mechanisms of PD-L1 expression in cancer cells. Cancer Immunol Immunother 2018;67(10):1481–9.
[24] Qin S, et al. Novel immune checkpoint targets: moving beyond PD-1 and CTLA-4. Mol Cancer 2019;18(1):155.
[25] Lee JB, Kim HR, Ha SJ. Immune checkpoint inhibitors in 10 years: contribution of basic research and clinical application in cancer immunotherapy. Immune Netw 2022;22(1):e2.
[26] Showalter A, et al. Cytokines in immunogenic cell death: Applications for cancer immunotherapy. Cytokine 2017;97:123–32.
[27] Eckert F, et al. Beyond checkpoint inhibition – immunotherapeutical strategies in combination with radiation. Clin Transl Radiat Oncol 2017;2:29–35.
[28] Kalbasi A, et al. Radiation and immunotherapy: a synergistic combination. J Clin Invest 2013;123(7):2756–63.
[29] Chiang SF, et al. Upregulation of tumor PD-L1 by neoadjuvant chemoradiotherapy (neoCRT) confers improved survival in patients with lymph node metastasis of locally advanced rectal cancers. Cancer Immunol Immunother 2018.
[30] Saigusa S, et al. Implication of programmed cell death ligand 1 expression in tumor recurrence and prognosis in rectal cancer with neoadjuvant chemoradiotherapy. Int J Clin Oncol 2016;21(5):946–52.
[31] Garon EB, et al. Pembrolizumab for the treatment of non-small-cell lung cancer. N Engl J Med 2015;372(21):2018–28.
[32] Kim JG, et al. Combination effect of epigenetic regulation and ionizing radiation in colorectal cancer cells. PLoS One 2014;9(8):e105405.
[33] Yang L, et al. Posttranscriptional control of PD-L1 expression by 17beta-estradiol via PI3K/Akt signaling pathway in ERalpha-positive cancer cell lines. Int J Gynecol Cancer 2017;27(2):196–205.
[34] Diskin B, et al. PD-L1 engagement on T cells promotes self-tolerance and suppression of neighboring macrophages and effector T cells in cancer. Nat Immunol 2020;21(4):442–54.
[35] Jiang Y, Li Y, Zhu B. T-cell exhaustion in the tumor microenvironment. Cell Death Dis 2015;6(6):e1792.
[36] Wu CT, et al. The role of PD-L1 in the radiation response and clinical outcome for bladder cancer. Sci Rep 2016;6:19740.
[37] Miyamoto Y, et al. Emerging evidence of immunotherapy for colorectal cancer. Ann Gastroenterol Surg 2023;7(2):216–24.
[38] Lenschow DJ, et al. Expression and functional significance of an additional ligand for CTLA-4. Proc Natl Acad Sci USA 1993;90(23):11054–8.
[39] Neefjes J, et al. Towards a systems understanding of MHC class I and MHC class II antigen presentation. Nat Rev Immunol 2011;11(12):823–36.
[40] Michelakos T, et al. Differential role of HLA-A and HLA-B, C expression levels as prognostic markers in colon and rectal cancer. J Immunother Cancer 2022;10(3).
[41] Gorvel L, Olive D. Targeting the “PVR-TIGIT axis” with immune checkpoint therapies. F1000Res 2020;9.
[42] Zheng Q, et al. CD155 knockdown promotes apoptosis via AKT/Bcl-2/Bax in colon cancer cells. J Cell Mol Med 2018;22(1):131–40.
[43] Vilar E, Gruber SB. Microsatellite instability in colorectal cancer-the stable evidence. Nat Rev Clin Oncol 2010;7(3):153–62.
[44] Hasan S, et al. Microsatellite instability (MSI) as an independent predictor of pathologic complete response (PCR) in locally advanced rectal cancer: a national cancer database (NCDB) analysis. Ann Surg 2018.
[45] Franchitto A, et al. The mammalian mismatch repair protein MSH2 is required for correct MRE11 and RAD51 relocalization and for efficient cell cycle arrest induced by ionizing radiation in G2 phase. Oncogene 2003;22(14):2110–20.
[46] Barwell J, et al. Biallelic mutation of MSH2 in primary human cells is associated with sensitivity to irradiation and altered RAD51 foci kinetics. J Med Genet 2007;44(8):516–20.
[47] Shin JS, et al. Radiotherapy response in microsatellite instability related rectal cancer. Korean J Pathol 2013;47(1):1–8.
[48] Charara M, et al. Microsatellite status and cell cycle associated markers in rectal cancer patients undergoing a combined regimen of 5-FU and CPT-11 chemotherapy and radiotherapy. Anticancer Res 2004;24(5B):3161–7.